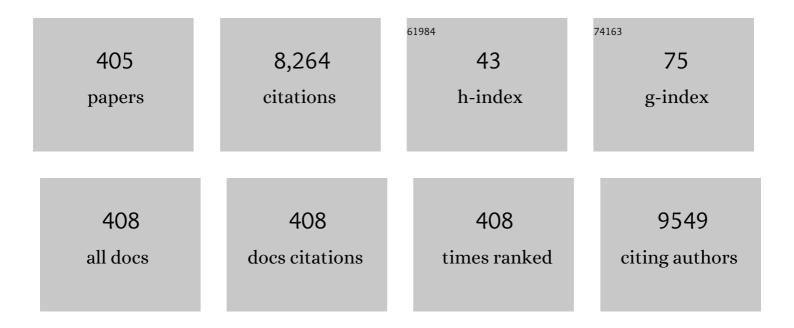
Harri Lipsanen

List of Publications by Year in descending order

Source: https://exaly.com/author-pdf/8371996/publications.pdf Version: 2024-02-01



#	Article	lF	CITATIONS
1	Probing Electronic States in Monolayer Semiconductors through Static and Transient Thirdâ€Harmonic Spectroscopies. Advanced Materials, 2022, 34, e2107104.	21.0	10
2	Enhanced terahertz emission from mushroom-shaped InAs nanowire network induced by linear and nonlinear optical effects. Nanotechnology, 2022, 33, 085207.	2.6	4
3	Femtosecond Mode-Locked Yb:KYW Laser Based on InP Nanowire Saturable Absorber. IEEE Photonics Technology Letters, 2022, 34, 247-250.	2.5	5
4	InSb Nanowire Direct Growth on Plastic for Monolithic Flexible Device Fabrication. ACS Applied Electronic Materials, 2022, 4, 539-545.	4.3	1
5	WITio: A MATLAB data evaluation toolbox to script broader insights into big data from WITec microscopes. SoftwareX, 2022, 18, 101009.	2.6	2
6	Direct GaAs Nanowire Growth and Monolithic Lightâ€Emitting Diode Fabrication on Flexible Plastic Substrates. Advanced Photonics Research, 2022, 3, .	3.6	4
7	Engineering the Dipole Orientation and Symmetry Breaking with Mixedâ€Đimensional Heterostructures. Advanced Science, 2022, 9, e2200082.	11.2	8
8	Designing outcoupling of light from nanostructured emitter in stratified medium with parasitic absorption. Journal of Applied Physics, 2022, 131, 223104.	2.5	0
9	Inducing Strong Light–Matter Coupling and Optical Anisotropy in Monolayer MoS ₂ with High Refractive Index Nanowire. ACS Applied Materials & Interfaces, 2022, 14, 31140-31147.	8.0	4
10	GaAs surface passivation for InAs/GaAs quantum dot based nanophotonic devices. Nanotechnology, 2021, 32, 130001.	2.6	7
11	Deterministic Modification of CVD Grown Monolayer MoS ₂ with Optical Pulses. Advanced Materials Interfaces, 2021, 8, 2002119.	3.7	6
12	Symmetry Reduction in FEM Optics Modeling of Single and Periodic Nanostructures. Symmetry, 2021, 13, 752.	2.2	2
13	Applied electromagnetic optics simulations for nanophotonics. Journal of Applied Physics, 2021, 129, .	2.5	18
14	Optical Modification of Monolayer MoS ₂ : Deterministic Modification of CVD Grown Monolayer MoS ₂ with Optical Pulses (Adv. Mater. Interfaces 10/2021). Advanced Materials Interfaces, 2021, 8, 2170056.	3.7	0
15	All-parylene flexible wafer-scale graphene thin film transistor. Applied Surface Science, 2021, 551, 149410.	6.1	14
16	Graphene/Bi2Se3 Heterojunction Phototransistor Using Photogating Effect Modulated by Tunable Tunneling Resistance. , 2021, , .		1
17	Effect of crystal structure on the Young's modulus of GaP nanowires. Nanotechnology, 2021, 32, 385706.	2.6	4
18	Giant All-Optical Modulation of Second-Harmonic Generation Mediated by Dark Excitons. ACS	6.6	11

#	Article	IF	CITATIONS
19	Ultrafast carrier dynamics and nonlinear optical response of InAsP nanowires. Photonics Research, 2021, 9, 1811.	7.0	5
20	Mechanical and optical properties of as-grown and thermally annealed titanium dioxide from titanium tetrachloride and water by atomic layer deposition. Thin Solid Films, 2021, 732, 138758.	1.8	17
21	Single-step chemical vapour deposition of anti-pyramid MoS ₂ /WS ₂ vertical heterostructures. Nanoscale, 2021, 13, 4537-4542.	5.6	17
22	Trends in Carbon, Oxygen, and Nitrogen Core in the X-ray Absorption Spectroscopy of Carbon Nanomaterials: A Guide for the Perplexed. Journal of Physical Chemistry C, 2021, 125, 973-988.	3.1	30
23	Multilayer MoTe ₂ Fieldâ€Effect Transistor at High Temperatures. Advanced Materials Interfaces, 2021, 8, 2100950.	3.7	14
24	Tuning of Emission Wavelength of CaS:Eu by Addition of Oxygen Using Atomic Layer Deposition. Materials, 2021, 14, 5966.	2.9	2
25	Grass-like alumina coated window harnesses the full omnidirectional potential of black silicon photodiodes. Applied Optics, 2021, 60, 10415.	1.8	3
26	Optical amplification by surface-plasmon-resonant Au grating substrates: Monolayer MoS2 with 170-fold second harmonic generation and 3-fold (off-resonance) Raman scattering. Superlattices and Microstructures, 2021, 160, 107077.	3.1	4
27	Tunable Quantum Tunneling through a Graphene/Bi ₂ Se ₃ Heterointerface for the Hybrid Photodetection Mechanism. ACS Applied Materials & Interfaces, 2021, 13, 58927-58935.	8.0	10
28	Tailoring the longitudinal electric fields of high-order laser beams and their direct verification in three dimensions. Optics Communications, 2020, 459, 124894.	2.1	3
29	High performance complementary WS ₂ devices with hybrid Gr/Ni contacts. Nanoscale, 2020, 12, 21280-21290.	5.6	27
30	Superhydrophobic Antireflection Coating on Glass Using Grass-like Alumina and Fluoropolymer. ACS Applied Materials & Interfaces, 2020, 12, 49957-49962.	8.0	51
31	Hybrid GaAs nanowire-polymer device on glass: Al-doped ZnO (AZO) as transparent conductive oxide for nanowire based photovoltaic applications. Journal of Crystal Growth, 2020, 548, 125840.	1.5	4
32	Review of fabrication methods of large-area transparent graphene electrodes for industry. Frontiers of Optoelectronics, 2020, 13, 91-113.	3.7	31
33	Fabrication-friendly polarization-sensitive plasmonic grating for optimal surface-enhanced Raman spectroscopy. Journal of the European Optical Society-Rapid Publications, 2020, 16, .	1.9	2
34	Nanowire Oligomer Waveguide Modes towards Reduced Lasing Threshold. Materials, 2020, 13, 5510.	2.9	2
35	Experimental Study and Simulation of the Spectral Characteristics of LED Heterostructures with an InAs Active Region. Technical Physics Letters, 2020, 46, 150-153.	0.7	2
36	Direct Growth of Light-Emitting Ill–V Nanowires on Flexible Plastic Substrates. ACS Nano, 2020, 14, 7484-7491.	14.6	24

#	Article	IF	CITATIONS
37	Management of light and scattering in InP NWs by dielectric polymer shell. Nanotechnology, 2020, 31, 384003.	2.6	3
38	Metalorganic vapor phase epitaxy of wurtzite InP nanowires on GaN. Applied Physics Letters, 2020, 116, 093101.	3.3	2
39	Geometry Tailoring of Emission from Semiconductor Nanowires and Nanocones. Photonics, 2020, 7, 23.	2.0	10
40	Production and processing of graphene and related materials. 2D Materials, 2020, 7, 022001.	4.4	333
41	Photodegradation of surface passivated GaAs nanowires. Journal of Physics: Conference Series, 2020, 1461, 012002.	0.4	1
42	Comparison of absorption simulation in semiconductor nanowire and nanocone arrays with the Fourier modal method, the finite element method, and the finite-difference time-domain method. Nano Express, 2020, 1, 030034.	2.4	13
43	Erbium-doped hybrid waveguide amplifiers with net optical gain on a fully industrial 300 mm silicon nitride photonic platform. Optics Express, 2020, 28, 27919.	3.4	20
44	Nonlinear optical absorption properties of InP nanowires and applications as a saturable absorber. Photonics Research, 2020, 8, 1035.	7.0	10
45	Nanowire-assisted microcavity in a photonic crystal waveguide and the enabled high-efficiency optical frequency conversions. Photonics Research, 2020, 8, 1734.	7.0	1
46	InAs-Nanowire-Based Broadband Ultrafast Optical Switch. Journal of Physical Chemistry Letters, 2019, 10, 4429-4436.	4.6	18
47	Growth of GaAs nanowire–graphite nanoplatelet hybrid structures. CrystEngComm, 2019, 21, 6165-6172.	2.6	5
48	Absorption modeling with FMM, FEM and FDT. , 2019, , .		1
49	Enhanced Tunneling in a Hybrid of Single-Walled Carbon Nanotubes and Graphene. ACS Nano, 2019, 13, 11522-11529.	14.6	23
50	Ultra-high on-chip optical gain in erbium-based hybrid slot waveguides. Nature Communications, 2019, 10, 432.	12.8	100
51	Aluminum Nitride Transition Layer for Power Electronics Applications Grown by Plasma-Enhanced Atomic Layer Deposition. Materials, 2019, 12, 406.	2.9	17
52	High photoresponsivity and broadband photodetection with a band-engineered WSe ₂ /SnSe ₂ heterostructure. Nanoscale, 2019, 11, 3240-3247.	5.6	84
53	Single-photon sources with quantum dots in Ill–V nanowires. Nanophotonics, 2019, 8, 747-769.	6.0	47
54	Determination of Young's Modulus of Wurtzite Ill–V Nanowires by the Methods of Scanning Probe Microscopy. Journal of Surface Investigation, 2019, 13, 53-55.	0.5	0

#	Article	IF	CITATIONS
55	Site-specific growth of oriented ZnO nanocrystal arrays. Beilstein Journal of Nanotechnology, 2019, 10, 274-280.	2.8	2
56	Low-Temperature Plasma-Enhanced Atomic Layer Deposition of SiO2 Using Carbon Dioxide. Nanoscale Research Letters, 2019, 14, 55.	5.7	7
57	Light-emitting InAs nanowires grown by MOVPE directly on flexible plastic substrates. , 2019, , .		0
58	Thermal conductivity suppression in GaAs–AlAs core–shell nanowire arrays. Nanoscale, 2019, 11, 20507-20513.	5.6	9
59	Title is missing!. Chinese Optics Letters, 2019, 17, 062301.	2.9	2
60	Comparison of FMM, FEM and FDTD for Absorption Modeling of Nanostructured Solar Cells and Photodetectors. , 2019, , .		0
61	Enhanced optical properties of InP nanowires by conformal polymer coating. , 2019, , .		0
62	Surface potential response from GaP nanowires synthesized with mixed crystal phases. Journal of Physics: Conference Series, 2019, 1400, 044018.	0.4	0
63	Ultrafast Dynamics of Photoinduced Electron–Hole Plasma in Semiconductor Nanowires. Semiconductors, 2018, 52, 19-23.	0.5	0
64	Ill–V nanowires on black silicon and low-temperature growth of self-catalyzed rectangular InAs NWs. Scientific Reports, 2018, 8, 6410.	3.3	11
65	Effect of Surface Wear on Corrosion Protection of Steel by CrN Coatings Sealed with Atomic Layer Deposition. ACS Omega, 2018, 3, 1791-1800.	3.5	18
66	Atomic layer deposition of AlN from AlCl3 using NH3 and Ar/NH3 plasma. Journal of Vacuum Science and Technology A: Vacuum, Surfaces and Films, 2018, 36, .	2.1	19
67	Tribological properties of thin films made by atomic layer deposition sliding against silicon. Journal of Vacuum Science and Technology A: Vacuum, Surfaces and Films, 2018, 36, .	2.1	7
68	Lifetimes of the Vibrational States of DNA Molecules in Functionalized Complexes of Semiconductor Quantum Dots. Technical Physics Letters, 2018, 44, 70-72.	0.7	4
69	Nonlinear Optics with 2D Layered Materials. Advanced Materials, 2018, 30, e1705963.	21.0	485
70	Transfer and patterning of chemical vapor deposited graphene by a multifunctional polymer film. Applied Physics Letters, 2018, 112, .	3.3	7
71	New method for MBE growth of GaAs nanowires on silicon using colloidal Au nanoparticles. Nanotechnology, 2018, 29, 045602.	2.6	6
72	Optical Properties of Bulk Gallium Oxide Grown from the Melt. Reviews on Advanced Materials Science, 2018, 57, 97-103.	3.3	4

#	Article	IF	CITATIONS
73	Coherent Electron Transport in Metamaterials of Integrated Semiconductor Quantum Dots and Biomolecules for Medical Imaging Applications. , 2018, , .		0
74	A MoSe ₂ /WSe ₂ Heterojunctionâ€Based Photodetector at Telecommunication Wavelengths. Advanced Functional Materials, 2018, 28, 1804388.	14.9	95
75	Influence of plasma parameters on the properties of ultrathin Al2O3 films prepared by plasma enhanced atomic layer deposition below 100 °C for moisture barrier applications. Japanese Journal of Applied Physics, 2018, 57, 125502.	1.5	16
76	Optical harmonic generation in monolayer group-VI transition metal dichalcogenides. Physical Review B, 2018, 98, .	3.2	92
77	Wide-band †black silicon' with atomic layer deposited NbN. Nanotechnology, 2018, 29, 335303.	2.6	5
78	Active synchronization and modulation of fiber lasers with a graphene electro-optic modulator. Optics Letters, 2018, 43, 3497.	3.3	12
79	Nanowire network–based multifunctional all-optical logic gates. Science Advances, 2018, 4, eaar7954.	10.3	51
80	Identifying threading dislocation types in ammonothermally grown bulk <mml:math xmlns:mml="http://www.w3.org/1998/Math/MathML" altimg="si1.gif" overflow="scroll"><mml:mrow><mml:mi>α</mml:mi></mml:mrow>-GaN by confocal Raman 3-D imaging of volumetric stress distribution. Journal of Crystal Growth, 2018, 499, 47-54.</mml:math 	1.5	12
81	Photoresponse of Graphene-Gated Graphene-GaSe Heterojunction Devices. ACS Applied Nano Materials, 2018, 1, 3895-3902.	5.0	23
82	Comparison of mechanical properties and composition of magnetron sputter and plasma enhanced atomic layer deposition aluminum nitride films. Journal of Vacuum Science and Technology A: Vacuum, Surfaces and Films, 2018, 36, .	2.1	10
83	Lowâ€Power Continuousâ€Wave Second Harmonic Generation in Semiconductor Nanowires. Laser and Photonics Reviews, 2018, 12, 1800126.	8.7	6
84	Nonlinear Optics: Nonlinear Optics with 2D Layered Materials (Adv. Mater. 24/2018). Advanced Materials, 2018, 30, 1870172.	21.0	8
85	Demonstration of longitudinally polarized optical needles. Optics Express, 2018, 26, 27572.	3.4	29
86	Corrosion protection of steel with multilayer coatings: Improving the sealing properties of physical vapor deposition CrN coatings with Al 2 O 3 /TiO 2 atomic layer deposition nanolaminates. Thin Solid Films, 2017, 627, 59-68.	1.8	32
87	Rapid and Large-Area Characterization of Exfoliated Black Phosphorus Using Third-Harmonic Generation Microscopy. Journal of Physical Chemistry Letters, 2017, 8, 1343-1350.	4.6	68
88	Graphene actively Q-switched lasers. 2D Materials, 2017, 4, 025095.	4.4	34
89	Crystal quality of two-dimensional gallium telluride and gallium selenide using Raman fingerprint. AIP Advances, 2017, 7, .	1.3	43
90	Tailorable secondâ€harmonic generation from an individual nanowire using spatially phaseâ€shaped beams. Laser and Photonics Reviews, 2017, 11, 1600175.	8.7	23

#	Article	IF	CITATIONS
91	Direct transfer of wafer-scale graphene films. 2D Materials, 2017, 4, 035004.	4.4	29
92	Young's Modulus of Wurtzite and Zinc Blende InP Nanowires. Nano Letters, 2017, 17, 3441-3446.	9.1	30
93	New Approach for Thickness Determination of Solution-Deposited Graphene Thin Films. ACS Omega, 2017, 2, 2630-2638.	3.5	8
94	Nanowire encapsulation with polymer for electrical isolation and enhanced optical properties. Nano Research, 2017, 10, 2657-2666.	10.4	16
95	Aluminum oxide/titanium dioxide nanolaminates grown by atomic layer deposition: Growth and mechanical properties. Journal of Vacuum Science and Technology A: Vacuum, Surfaces and Films, 2017, 35, .	2.1	38
96	Review Article: Recommended reading list of early publications on atomic layer deposition—Outcome of the "Virtual Project on the History of ALD― Journal of Vacuum Science and Technology A: Vacuum, Surfaces and Films, 2017, 35, .	2.1	65
97	l–V curve hysteresis induced by gate-free charging of GaAs nanowires' surface oxide. Applied Physics Letters, 2017, 111, 132104.	3.3	9
98	Ultra-strong nonlinear optical processes and trigonal warping in MoS2 layers. Nature Communications, 2017, 8, 893.	12.8	177
99	Versatile Water-Based Transfer of Large-Area Graphene Films onto Flexible Substrates. MRS Advances, 2017, 2, 3749-3754.	0.9	2
100	Probing the longitudinal electric field of Bessel beams using second-harmonic generation from nano-objects. Journal of Optics (United Kingdom), 2017, 19, 084011.	2.2	3
101	Low temperature and high quality atomic layer deposition HfO <inf>2</inf> coatings. , 2017, , ·		1
102	MBE growth of nanowires using colloidal Ag nanoparticles. Journal of Physics: Conference Series, 2017, 864, 012010.	0.4	2
103	Scaling of graphene field-effect transistors supported on hexagonal boron nitride: radio-frequency stability as a limiting factor. Nanotechnology, 2017, 28, 485203.	2.6	15
104	Optically excited THz generation from ordered arrays of GaAs nanowires. Procedia Engineering, 2017, 201, 100-104.	1.2	1
105	Spontaneous and stimulated emission in InAsSb-based LED heterostructures. Infrared Physics and Technology, 2017, 85, 246-250.	2.9	14
106	Electroluminescence of InAs/InAs(Sb)/InAsSbP LED heterostructures in the temperature range 4.2–300 K. Semiconductors, 2017, 51, 239-244.	0.5	5
107	Rapid visualization of grain boundaries in monolayer MoS2 by multiphoton microscopy. Nature Communications, 2017, 8, 15714.	12.8	120
108	Measurement of Nanowire Optical Modes Using Cross-Polarization Microscopy. Scientific Reports, 2017, 7, 17790.	3.3	6

#	Article	IF	CITATIONS
109	Fast dynamics of photoexcited electron-hole plasma in GaAs nanowires. , 2017, , .		0
110	Nonlinear imaging of nanostructures using beams with binary phase modulation. Optics Express, 2017, 25, 10441.	3.4	3
111	Nonlinear microscopy using cylindrical vector beams: Applications to three-dimensional imaging of nanostructures. Optics Express, 2017, 25, 12463.	3.4	26
112	Detection of Raman Scattering Spectra of High Spectral Resolution in Short Oligonucleotides: Compared with the Full-Length DNA Spectra. Herald of the Bauman Moscow State Technical University, Series Natural Sciences, 2017, , .	0.5	0
113	Growth and properties of selfâ€catalyzed (In,Mn)As nanowires. Physica Status Solidi - Rapid Research Letters, 2016, 10, 554-557.	2.4	3
114	Tunable Graphene–GaSe Dual Heterojunction Device. Advanced Materials, 2016, 28, 1845-1852.	21.0	90
115	Direct measurement of elastic modulus of InP nanowires with Scanning Probe Microscopy in PeakForce QNM mode. Journal of Physics: Conference Series, 2016, 769, 012029.	0.4	3
116	Protective capping and surface passivation of III-V nanowires by atomic layer deposition. AIP Advances, 2016, 6, .	1.3	29
117	Surface passivation of GaAs nanowires by the atomic layer deposition of AlN. Semiconductors, 2016, 50, 1619-1621.	0.5	1
118	Structural and chemical analysis of annealed plasma-enhanced atomic layer deposition aluminum nitride films. Journal of Vacuum Science and Technology A: Vacuum, Surfaces and Films, 2016, 34, .	2.1	22
119	Second and third harmonic generation in few-layer gallium telluride characterized by multiphoton microscopy. Applied Physics Letters, 2016, 108, .	3.3	58
120	Resonant features of the terahertz generation in semiconductor nanowires. Semiconductors, 2016, 50, 1561-1565.	0.5	5
121	Efficient terahertz generation by ordered arrays of GaAs nanowires. , 2016, , .		1
122	Black phosphorus polycarbonate polymer composite for pulsed fibre lasers. Applied Materials Today, 2016, 4, 17-23.	4.3	87
123	Optical characterization of directly deposited graphene on a dielectric substrate. Optics Express, 2016, 24, 2965.	3.4	5
124	TEM study of defect structure of GaN epitaxial films grown on GaN/Al2O3 substrates with buried column pattern. Journal of Crystal Growth, 2016, 445, 30-36.	1.5	5
125	Thermal conductivity of amorphous Al ₂ O ₃ /TiO ₂ nanolaminates deposited by atomic layer deposition. Nanotechnology, 2016, 27, 445704.	2.6	27
126	Atomic Layer Engineering of Er-Ion Distribution in Highly Doped Er:Al ₂ O ₃ for Photoluminescence Enhancement. ACS Photonics, 2016, 3, 2040-2048.	6.6	27

#	Article	IF	CITATIONS
127	Lithography-free shell-substrate isolation for core–shell GaAs nanowires. Nanotechnology, 2016, 27, 275603.	2.6	1
128	Synthesis and properties of ultra-long InP nanowires on glass. Nanotechnology, 2016, 27, 505606.	2.6	7
129	Direct observation of confined acoustic phonon polarization branches in free-standing semiconductor nanowires. Nature Communications, 2016, 7, 13400.	12.8	71
130	Pyrolytic carbon coated black silicon. Scientific Reports, 2016, 6, 25922.	3.3	12
131	Integration of atomic layer deposited nanolaminates on silicon waveguides (Conference) Tj ETQq1 1 0.784314 rg	gBT /Over	lock 10 Tf 50
132	Atomic layer deposition of highly doped Er:Al2O3 and Tm:Al2O3 for silicon-based waveguide amplifiers (Conference Presentation). , 2016, , .		0
133	Synchrotron X-ray diffraction topography study of bonding-induced strain in silicon-on-insulator wafers. Thin Solid Films, 2016, 603, 435-440.	1.8	2
134	Enhancement of the photoluminescence in Er-doped Al2O3fabricated by atomic layer deposition. , 2016,		1
135	A technique for large-area position-controlled growth of GaAs nanowire arrays. Nanotechnology, 2016, 27, 135601.	2.6	9
136	Direct comparison of second and third harmonic generation in mono- and few-layer MX2 (M=Mo,W;) Tj ETQq0 0	0 rgBT /C	verlock 10 Tf
137	Influence of surface passivation on electric properties of individual GaAs nanowires studied by current–voltage AFM measurements. Lithuanian Journal of Physics, 2016, 56, .	0.4	11
138	Nonlinear microscopy of nano-objects using excitation beam profiles with engineered phase jumps. , 2016, , .		0
139	Spectral characteristics of mid-infrared light-emitting diodes based on InAs(Sb,P). Scientific and Technical Journal of Information Technologies, Mechanics and Optics, 2016, , 76-84.	0.2	1
140	Polarization and Thickness Dependent Absorption Properties of Black Phosphorus: New Saturable Absorber for Ultrafast Pulse Generation. Scientific Reports, 2015, 5, 15899.	3.3	268
141	Wafer-scale self-organized InP nanopillars with controlled orientation for photovoltaic devices. Nanotechnology, 2015, 26, 415304.	2.6	13
142	Generation of terahertz radiation in ordered arrays of GaAs nanowires. Applied Physics Letters, 2015, 106, .	3.3	21
143	Observation of linear I-V curves on vertical GaAs nanowires with atomic force microscope. Journal of Physics: Conference Series, 2015, 661, 012031.	0.4	3
144	Broadband laser polarization control with aligned carbon nanotubes. Nanoscale, 2015, 7, 11199-11205.	5.6	14

#	Article	IF	CITATIONS
145	A physics-based model of gate-tunable metal–graphene contact resistance benchmarked against experimental data. 2D Materials, 2015, 2, 025006.	4.4	30
146	Investigation of Second- and Third-Harmonic Generation in Few-Layer Gallium Selenide by Multiphoton Microscopy. Scientific Reports, 2015, 5, 10334.	3.3	98
147	Second-Harmonic Generation Imaging of Semiconductor Nanowires with Focused Vector Beams. Nano Letters, 2015, 15, 1564-1569.	9.1	66
148	Fabrication of Dual-Type Nanowire Arrays on a Single Substrate. Nano Letters, 2015, 15, 1679-1683.	9.1	9
149	Processing and characterization of epitaxial GaAs radiation detectors. Nuclear Instruments and Methods in Physics Research, Section A: Accelerators, Spectrometers, Detectors and Associated Equipment, 2015, 796, 51-55.	1.6	8
150	Solubility of Boron, Carbon, and Nitrogen in Transition Metals: Getting Insight into Trends from First-Principles Calculations. Journal of Physical Chemistry Letters, 2015, 6, 3263-3268.	4.6	50
151	Optical limiting in solutions of InP and GaAs nanowires and hybrid systems based on such nanocrystals. Technical Physics Letters, 2015, 41, 120-123.	0.7	3
152	All-Graphene Three-Terminal-Junction Field-Effect Devices as Rectifiers and Inverters. ACS Nano, 2015, 9, 5666-5674.	14.6	14
153	Slot waveguide ring resonators coated by an atomic layer deposited organic/inorganic nanolaminate. Optics Express, 2015, 23, 26940.	3.4	14
154	Nanotribological, nanomechanical and interfacial characterization of atomic layer deposited TiO2 on a silicon substrate. Wear, 2015, 342-343, 270-278.	3.1	13
155	The effect of resonant Mie absorption under THz radiation emission in semiconductor nanowires. Optics and Spectroscopy (English Translation of Optika I Spektroskopiya), 2015, 119, 754-758.	0.6	1
156	Observing grain boundaries in monolayer molybdenum disulphide by multiphoton microscopy. , 2015, , .		0
157	Resonant raman scattering in complexes of nc-Si/SiO2 quantum dots and oligonucleotides. Technical Physics Letters, 2014, 40, 1035-1037.	0.7	2
158	Leakage currents of large area InP/InGaAs heterostructures. Materials Research Society Symposia Proceedings, 2014, 1635, 75-81.	0.1	0
159	Effects of Zn doping on GaAs nanowires. , 2014, , .		4
160	Impact of ALD grown passivation layers on silicon nitride based integrated optic devices for very-near-infrared wavelengths. Optics Express, 2014, 22, 5684.	3.4	24
161	Radiation detectors fabricated on high-purity GaAs epitaxial materials. Journal of Instrumentation, 2014, 9, C12024-C12024.	1.2	1
162	Stress distribution in GaN nanopillars using confocal Raman mapping technique. Applied Physics Letters, 2014, 104, 151906.	3.3	5

#	Article	IF	CITATIONS
163	Yield and leakage currents of large area lattice matched InP/InGaAs heterostructures. Journal of Applied Physics, 2014, 116, .	2.5	4
164	Strong surface passivation of GaAs nanowires with ultrathin InP and GaP capping layers. Applied Physics Letters, 2014, 105, .	3.3	31
165	Nanolaminate structures fabricated by ALD for reducing propagation losses and enhancing the third-order optical nonlinearities. Proceedings of SPIE, 2014, , .	0.8	6
166	Reflectance measurements of triangular lattice GaAs nanowire arrays. , 2014, , .		0
167	Exceptionally strong and robust millimeter-scale graphene–alumina composite membranes. Nanotechnology, 2014, 25, 355701.	2.6	4
168	Effect of growth temperature on the epitaxial growth of ZnO on GaN by ALD. Journal of Crystal Growth, 2014, 398, 18-22.	1.5	19
169	Aluminum oxide from trimethylaluminum and water by atomic layer deposition: The temperature dependence of residual stress, elastic modulus, hardness and adhesion. Thin Solid Films, 2014, 552, 124-135.	1.8	155
170	Improved SERS Intensity from Silverâ€Coated Black Silicon by Tuning Surface Plasmons. Advanced Materials Interfaces, 2014, 1, 1300008.	3.7	15
171	X-ray reflectivity characterization of atomic layer deposition Al2O3/TiO2 nanolaminates with ultrathin bilayers. Journal of Vacuum Science and Technology A: Vacuum, Surfaces and Films, 2014, 32, .	2.1	28
172	Thermal and plasma enhanced atomic layer deposition of SiO2 using commercial silicon precursors. Thin Solid Films, 2014, 558, 93-98.	1.8	66
173	Photo-induced electron transfer at nanostructured semiconductor–zinc porphyrin interface. Chemical Physics Letters, 2014, 592, 47-51.	2.6	12
174	Functionalization of nc-Si/SiO2 semiconductor quantum dots by oligonucleotides. Semiconductors, 2014, 48, 1485-1489.	0.5	2
175	Electrical detection of picosecond acoustic pulses in vertical transport devices with nanowires. Applied Physics Letters, 2014, 104, 062102.	3.3	2
176	Synchrotron radiation x-ray topography and defect selective etching analysis of threading dislocations in GaN. Journal of Applied Physics, 2014, 116, 083504.	2.5	37
177	Defect structure of a free standing GaN wafer grown by the ammonothermal method. Journal of Crystal Growth, 2014, 406, 72-77.	1.5	13
178	Large-area analysis of dislocations in ammonothermal GaN by synchrotron radiation X-ray topography. Applied Physics Express, 2014, 7, 091003.	2.4	20
179	Properties of atomic-layer-deposited ultra-thin AlN films on GaAs surfaces. Applied Surface Science, 2014, 314, 570-574.	6.1	4
180	Performance and Properties of Ultra-Thin Silicon Nitride X-ray Windows. IEEE Transactions on Nuclear Science, 2014, 61, 695-699.	2.0	15

#	Article	IF	CITATIONS
181	Substitutionality of nitrogen atoms and formation of nitrogen complexes and point defects in GaPN alloys. Journal Physics D: Applied Physics, 2014, 47, 075106.	2.8	12
182	Low-height sharp edged patterns for capillary self-alignment assisted hybrid microassembly. Journal of Micro-Bio Robotics, 2014, 9, 1-10.	2.1	17
183	Detection of high-resolution Raman spectra in short oligonucleotides. JETP Letters, 2014, 99, 373-377.	1.4	7
184	High-resolution Raman scattering in oligonucleotides. Physics of the Solid State, 2014, 56, 1273-1275.	0.6	3
185	High-resolution Raman scattering in oligonucleotides. Technical Physics Letters, 2014, 40, 340-342.	0.7	3
186	Ultrafast carrier dynamics in GaAs nanowires. Lithuanian Journal of Physics, 2014, 54, 41-45.	0.4	2
187	Aluminum-Induced Photoluminescence Red Shifts in Core–Shell GaAs/Al _{<i>x</i>} Ga _{1–<i>x</i>} As Nanowires. Nano Letters, 2013, 13, 3581-3588.	9.1	23
188	New method of determining the young's Modulus of (Ga,Mn)As nanowhiskers with a scanning electron microscope. Physics of the Solid State, 2013, 55, 2229-2233.	0.6	1
189	Rapid Large-Area Multiphoton Microscopy for Characterization of Graphene. ACS Nano, 2013, 7, 8441-8446.	14.6	81
190	Surface-Tension-Driven Self-Alignment of Microchips on Black-Silicon-Based Hybrid Template in Ambient Air. Journal of Microelectromechanical Systems, 2013, 22, 739-746.	2.5	18
191	Fabrication of GaN structures with embedded network of voids using pillar patterned GaN templates. Journal of Crystal Growth, 2013, 370, 42-45.	1.5	2
192	Evaluation of critical thickness of GaP0.98N0.02 layer on GaP substrate by synchrotron X-ray diffraction topography. Thin Solid Films, 2013, 534, 680-684.	1.8	5
193	Ultra-Thin Silicon Nitride X-Ray Windows. IEEE Transactions on Nuclear Science, 2013, 60, 1311-1314.	2.0	19
194	Temperature dependence of droop onset in optically pumped intrinsic InGaAs/InP heterostructures. Applied Physics Letters, 2013, 102, .	3.3	3
195	Photo-thermal chemical vapor deposition of graphene on copper. Carbon, 2013, 62, 43-50.	10.3	32
196	High-quality crystallinity controlled ALD TiO_2 for waveguiding applications. Optics Letters, 2013, 38, 3980.	3.3	22
197	Highly tunable local gate controlled complementary graphene device performing as inverter and voltage controlled resistor. Nanotechnology, 2013, 24, 395202.	2.6	7
198	Strain-compensated GaPN/GaP heterostructure on (0 0 1) silicon substrates for intermediate band solar cells. Journal Physics D: Applied Physics, 2013, 46, 165103.	2.8	10

#	Article	IF	CITATIONS
199	Carriers transport in GaAs nanowires. , 2013, , .		о
200	Stress distribution of GaN layer grown on micro-pillar patterned GaN templates. Applied Physics Letters, 2013, 103, .	3.3	12
201	Fabrication of large-area plasmonic nanostructures for surface enhanced fluorescence. , 2013, , .		1
202	GaAs nanowires grown on Al-doped ZnO buffer layer. Journal of Applied Physics, 2013, 114, .	2.5	8
203	Strong two-photon excitation fluorescence from GaAs and InP nanowires on glass substrate. , 2013, , .		О
204	Third-harmonic and multiphoton excitation fluorescence microscopy of single and few layer graphene. , 2013, , .		0
205	Influence of plasma chemistry on impurity incorporation in AlN prepared by plasma enhanced atomic layer deposition. Journal Physics D: Applied Physics, 2013, 46, 505502.	2.8	32
206	Analysis of Dislocations Generated during Metal–Organic Vapor Phase Epitaxy of GaN on Patterned Templates. Japanese Journal of Applied Physics, 2013, 52, 01AF01.	1.5	2
207	Ferromagnetic (Ga,Mn)As nanowires grown by Mn-assisted molecular beam epitaxy. Journal of Applied Physics, 2013, 113, .	2.5	13
208	(Invited) Self-Assembled Monolayers of Porphyrin Derivatives on Semiconductor Surfaces: Photoindued Reactions at the Interface. ECS Meeting Abstracts, 2013, , .	0.0	0
209	A novel all-vapor phase fabrication process for ytterbium-doped fibers with atomic layer deposition method. , 2013, , .		0
210	Growth of CVD graphene on copper by rapid thermal processing. Materials Research Society Symposia Proceedings, 2012, 1451, 27-32.	0.1	2
211	High- <i>k</i> GaAs metal insulator semiconductor capacitors passivated by <i>ex-situ</i> plasma-enhanced atomic layer deposited AlN for Fermi-level unpinning. Applied Physics Letters, 2012, 100, .	3.3	20
212	Comparison of ammonia plasma and AlN passivation by plasma-enhanced atomic layer deposition. Journal of Applied Physics, 2012, 111, .	2.5	9
213	Plasma etch characteristics of aluminum nitride mask layers grown by low-temperature plasma enhanced atomic layer deposition in SF6 based plasmas. Journal of Vacuum Science and Technology A: Vacuum, Surfaces and Films, 2012, 30, .	2.1	12
214	Structural study of GaP layers on misoriented silicon (001) substrates by transverse scan analysis. Journal of Applied Physics, 2012, 111, .	2.5	10
215	Surface-tension driven self-assembly of microchips on hydrophobic receptor sites with water using forced wetting. Applied Physics Letters, 2012, 101, 114105.	3.3	24
216	Photovoltaic properties of GaAsP core–shell nanowires on Si(001) substrate. Nanotechnology, 2012, 23, 265402.	2.6	45

#	Article	IF	CITATIONS
217	Analysis of threading dislocations in void shape controlled GaN re-grown on hexagonally patterned mask-less GaN. Journal of Crystal Growth, 2012, 344, 59-64.	1.5	14
218	Self-Assembled Porphyrins on Modified Zinc Oxide Nanorods: Development of Model Systems for Inorganic–Organic Semiconductor Interface Studies. Journal of Physical Chemistry C, 2012, 116, 2336-2343.	3.1	37
219	Enhancement of near-UV GaN LED light extraction efficiency by GaN/sapphire template patterning. Semiconductor Science and Technology, 2012, 27, 082002.	2.0	10
220	Graphene-enhanced Raman imaging of TiO ₂ nanoparticles. Nanotechnology, 2012, 23, 465703.	2.6	56
221	Electrical measurement of internal quantum efficiency and extraction efficiency of III-N light-emitting diodes. Applied Physics Letters, 2012, 101, .	3.3	33
222	High Quality GaAs Nanowires Grown on Glass Substrates. Nano Letters, 2012, 12, 1912-1918.	9.1	70
223	Synthesis of ZnO tetrapods for flexible and transparent UV sensors. Nanotechnology, 2012, 23, 095502.	2.6	40
224	Characterization of InGaAs/GaNAs strainâ€compensated quantum dot solar cells. Physica Status Solidi C: Current Topics in Solid State Physics, 2012, 9, 972-974.	0.8	3
225	Growth and characterization of GaP layers on silicon substrates by metalâ€organic vapour phase epitaxy. Physica Status Solidi C: Current Topics in Solid State Physics, 2012, 9, 1607-1609.	0.8	11
226	Effect of atomic-layer-deposited AlN on near-surface InGaAs/GaAs structures. Physica Status Solidi C: Current Topics in Solid State Physics, 2012, 9, 1560-1562.	0.8	1
227	Synchrotron radiation Xâ€ray topography and Xâ€ray diffraction of homoepitaxial GaN grown on ammonothermal GaN. Physica Status Solidi C: Current Topics in Solid State Physics, 2012, 9, 1630-1632.	0.8	7
228	MOCVD growth and characterization of nearâ€surface InGaN/GaN single quantum wells for nonâ€radiative coupling of optical excitations. Physica Status Solidi C: Current Topics in Solid State Physics, 2012, 9, 1667-1669.	0.8	4
229	Nonlinear behavior of three-terminal graphene junctions at room temperature. Nanotechnology, 2012, 23, 115201.	2.6	13
230	Formation of (Ga,Mn)As nanowires and study of their magnetic properties. Semiconductors, 2012, 46, 179-183.	0.5	11
231	Nd-doped Bismuth Titanate based ferroelectric field effect transistor: Design, fabrication, and optimization. , 2011, , .		0
232	Capillary-driven self-assembly of microchips on oleophilic/oleophobic patterned surface using adhesive droplet in ambient air. Applied Physics Letters, 2011, 99, 034104.	3.3	34
233	Electrical properties of CVD-graphene FETs. , 2011, , .		2
234	Temperature Dependence of Current-Voltage Characteristics of Auâ^•Ga[sub 0.51]In[sub 0.49]P Schottky Barrier Diodes. AIP Conference Proceedings, 2011, , .	0.4	10

#	Article	IF	CITATIONS
235	Temperature Dependence Of Current-Voltage Characteristics Of Auâ^•p-GaAsN Schottky Barrier Diodes, With Small N Content. , 2011, , .		1
236	A single-pixel wireless contact lens display. Journal of Micromechanics and Microengineering, 2011, 21, 125014.	2.6	121
237	Growth temperature dependence of the electrical and structural properties of epitaxial graphene on SiC(0001). Physica Status Solidi (B): Basic Research, 2011, 248, 1908-1914.	1.5	13
238	Xâ€ray diffraction study of GaN grown on patterned substrates. Physica Status Solidi C: Current Topics in Solid State Physics, 2011, 8, 1524-1527.	0.8	2
239	Patterning of sapphire/GaN substrates. Physica Status Solidi C: Current Topics in Solid State Physics, 2011, 8, 1509-1512.	0.8	11
240	TlBr purification and single crystal growth for the detector applications. Nuclear Instruments and Methods in Physics Research, Section A: Accelerators, Spectrometers, Detectors and Associated Equipment, 2011, 633, S72-S74.	1.6	4
241	Properties of AlN grown by plasma enhanced atomic layer deposition. Applied Surface Science, 2011, 257, 7827-7830.	6.1	112
242	Void shape control in GaN re-grown on hexagonally patterned mask-less GaN. Journal of Crystal Growth, 2011, 315, 188-191.	1.5	15
243	Inhomogeneous Barrier Height Analysis of (Ni/Au)–InAlGaN/GaN Schottky Barrier Diode. Japanese Journal of Applied Physics, 2011, 50, 030201.	1.5	10
244	Enhanced 1.3 µm luminescence from InGaAs self-assembled quantum dots with a GaAsN strain-compensating layer. Semiconductor Science and Technology, 2011, 26, 085029.	2.0	1
245	Building molecular surface gradients with electron beam lithography. Journal of Micromechanics and Microengineering, 2011, 21, 054025.	2.6	3
246	ATOMIC LAYER DEPOSITION HfO₂ FILM USED AS BUFFER LAYER OF THE Pt/(Bi_{0.95}Nd_{0.05})(Fe_{0.95}Mn_{0.05})O₃ CAPACITORS FOR FeFET APPLICATION. Journal of Advanced Dielectrics, 2011, 01, 369-377.	/HfO xs ub>	2 <b 6ub>/Si
247	Recent progress towards acoustically mediated carrier injection into individual nanostructures for single photon generation. Proceedings of SPIE, 2010, , .	0.8	1
248	Temperature Dependence Of Current-Voltage Characteristics Of Ptâ^•InN Schottky Barrier Diodes. AIP Conference Proceedings, 2010, , .	0.4	3
249	Emission of terahertz radiation from GaN under impact ionization of donors in an electric field. Bulletin of the Russian Academy of Sciences: Physics, 2010, 74, 86-88.	0.6	3
250	Influence of substrate temperature on the shape of GaAs nanowires grown by Au-assisted MOVPE. Journal of Crystal Growth, 2010, 312, 1676-1682.	1.5	11
251	GaAs surface passivation by plasma-enhanced atomic-layer-deposited aluminum nitride. Applied Surface Science, 2010, 256, 7434-7437.	6.1	43
252	Characterization of InGaN/GaN and AlGaN/GaN superlattices by X-ray diffraction and X-ray reflectivity measurements. Physica Status Solidi C: Current Topics in Solid State Physics, 2010, 7, 1790-1793.	0.8	4

#	Article	IF	CITATIONS
253	Forward Bias Capacitance-Voltage Measurements on Semiconductors Using Co-Planar Ohmic and Schottky Contacts in a Cylindrical Geometry. Journal of Nano Research, 2010, 12, 45-54.	0.8	2
254	GaAs Nanowire and Crystallite Growth on Amorphous Substrate from Metalorganic Precursors. Japanese Journal of Applied Physics, 2010, 49, 020213.	1.5	2
255	InGaN-based 405 nm near-ultraviolet light emitting diodes on pillar patterned sapphire substrates. CrystEngComm, 2010, 12, 3152.	2.6	13
256	Terahertz emission from GaN epilayers at lateral electric field. , 2010, , .		0
257	Substrate-patterning techniques for nitride growth. SPIE Newsroom, 2010, , .	0.1	0
258	Cascaded exciton emission of an individual strain-induced quantum dot. Applied Physics Letters, 2009, 95, 083122.	3.3	7
259	FABRICATION AND OPTICAL PROPERTIES OF METAL-COATED NON-CLOSE-PACKED COLLOIDAL CRYSTALS. Journal of Nonlinear Optical Physics and Materials, 2009, 18, 633-640.	1.8	0
260	Impurity breakdown and terahertz luminescence in n-GaN epilayers under external electric field. Journal of Applied Physics, 2009, 106, 123523.	2.5	26
261	Tunneling Explanation for the Temperature Dependence of Current–Voltage Characteristics of Pt/InN Schottky Barrier Diodes. Japanese Journal of Applied Physics, 2009, 48, 070201.	1.5	8
262	Atomic layer deposition of ytterbium oxide using -diketonate and ozone precursors. Applied Surface Science, 2009, 256, 847-851.	6.1	20
263	Characterization of TlBr for X-ray and Î ³ -ray detector applications. Nuclear Instruments and Methods in Physics Research, Section A: Accelerators, Spectrometers, Detectors and Associated Equipment, 2009, 607, 129-131.	1.6	7
264	Improvements and problems of Bridgman–Stockbarger method for fabrication of TlBr single crystal detectors. Nuclear Instruments and Methods in Physics Research, Section A: Accelerators, Spectrometers, Detectors and Associated Equipment, 2009, 607, 126-128.	1.6	8
265	An investigation of structural properties of GaN films grown on patterned sapphire substrates by MOVPE. Physica B: Condensed Matter, 2009, 404, 4911-4915.	2.7	8
266	Reduced photoluminescence from InGaN/GaN multiple quantum well structures following 40Mev iodine ion irradiation. Physica B: Condensed Matter, 2009, 404, 4925-4928.	2.7	10
267	Synchrotron topography and X-ray diffraction study of GaInP layers grown on GaAs/Ge. Journal of Crystal Growth, 2009, 311, 4619-4627.	1.5	10
268	Mechanistic investigation of ZnO nanowire growth. Applied Physics Letters, 2009, 95, 183114.	3.3	38
269	Self-assembled InAs island formation on GaAs (110) by metalorganic vapor phase epitaxy. Applied Surface Science, 2008, 254, 2072-2076.	6.1	10
270	In-situ optical reflectance and synchrotron X-ray topography study of defects in epitaxial dilute GaAsN on GaAs. Journal of Materials Science: Materials in Electronics, 2008, 19, 137-142.	2.2	4

#	Article	IF	CITATIONS
271	Study of composition control and capping of MOVPE grown InGaN/InxAlyGa1-x-yN MQW structures. Physica Status Solidi C: Current Topics in Solid State Physics, 2008, 5, 3020-3022.	0.8	0
272	MOVPE growth and characterization of InAlGaN films and InGaN/InAlGaN MQW structures. Journal of Crystal Growth, 2008, 310, 1777-1780.	1.5	13
273	Enhanced electroluminescence in 405nm InGaN/GaN LEDs by optimized electron blocking layer. Journal of Crystal Growth, 2008, 310, 5154-5157.	1.5	24
274	GaAs Medipix2 hybrid pixel detector. Nuclear Instruments and Methods in Physics Research, Section A: Accelerators, Spectrometers, Detectors and Associated Equipment, 2008, 591, 174-177.	1.6	11
275	Passivation of GaAs surface by atomic-layer-deposited titanium nitride. Applied Surface Science, 2008, 254, 5385-5389.	6.1	18
276	Properties, applications and fabrication of photonic crystals with ring-shaped holes in silicon-on-insulator. Photonics and Nanostructures - Fundamentals and Applications, 2008, 6, 42-46.	2.0	27
277	Efficient light coupling into a photonic crystal waveguide with flatband slow mode. Photonics and Nanostructures - Fundamentals and Applications, 2008, 6, 127-133.	2.0	5
278	Synchrotron X-ray topography and electrical characterization of epitaxial GaAs p–i–n structures. Nuclear Instruments and Methods in Physics Research, Section A: Accelerators, Spectrometers, Detectors and Associated Equipment, 2008, 591, 192-195.	1.6	1
279	Carrier Dynamics in Strain Induced Quantum Dots Modeled by Rate Equations and Gaussian Excitation Beam Distribution. Japanese Journal of Applied Physics, 2008, 47, 5499-5502.	1.5	0
280	Novel method for error limit determination in x-ray reflectivity analysis. Journal Physics D: Applied Physics, 2008, 41, 115302.	2.8	8
281	Slow-light photonic crystal waveguides with ring-shaped holes on silicon-on-insulator. Proceedings of SPIE, 2008, , .	0.8	0
282	Amorphous silicon optical waveguides and Bragg mirrors. , 2008, , .		5
283	Genetic algorithm using independent component analysis in x-ray reflectivity curve fitting of periodic layer structures. Journal Physics D: Applied Physics, 2007, 40, 6000-6004.	2.8	16
284	Fitness function and nonunique solutions in x-ray reflectivity curve fitting: crosserror between surface roughness and mass density. Journal Physics D: Applied Physics, 2007, 40, 4259-4263.	2.8	12
285	Nonlinear fitness–space–structure adaptation and principal component analysis in genetic algorithms: an application to x-ray reflectivity analysis. Journal Physics D: Applied Physics, 2007, 40, 215-218.	2.8	16
286	Accuracy in x-ray reflectivity analysis. Journal Physics D: Applied Physics, 2007, 40, 7497-7501.	2.8	7
287	In situ determination of InGaAs and GaAsN composition in multiquantum-well structures. Journal of Applied Physics, 2007, 101, 033533.	2.5	3
288	Tensile-strained GaAsN quantum dots on InP. Applied Physics Letters, 2007, 90, 172110.	3.3	5

#	Article	IF	CITATIONS
289	Effect of substrate orientation on the catalyst-free growth of InP nanowires. Nanotechnology, 2007, 18, 155301.	2.6	37
290	Dispersion engineering of photonic crystal waveguides with ring-shaped holes. Optics Express, 2007, 15, 8323.	3.4	112
291	Enhanced luminescence from catalyst-free grown InP nanowires. Applied Physics Letters, 2007, 90, 033101.	3.3	43
292	Nine-fold photoluminescence enhancement using photonic crystals with graphite lattice. Indium Phosphide and Related Materials Conference (IPRM), IEEE International Conference on, 2007, , .	0.0	0
293	Noncovalent attachment of pyro-pheophorbidea to a carbon nanotube. Chemical Communications, 2007, , 519-521.	4.1	50
294	Slow light propagation in photonic crystal waveguides with ring-shaped holes. Journal of Optics, 2007, 9, S415-S418.	1.5	24
295	GaAs surface passivation by ultra-thin epitaxial GaP layer and surface As–P exchange. Applied Surface Science, 2007, 253, 6232-6235.	6.1	6
296	Comparison of and as carrier gas in MOVPE growth of InGaAsN quantum wells. Journal of Crystal Growth, 2007, 298, 536-539.	1.5	5
297	Catalyst-free fabrication of InP and InP(N) nanowires by metalorganic vapor phase epitaxy. Journal of Crystal Growth, 2007, 298, 640-643.	1.5	10
298	Reduction of threading dislocation density in Al0.12Ga0.88N epilayers by a multistep technique. Journal of Crystal Growth, 2007, 298, 276-280.	1.5	4
299	Effect of growth conditions on electrical properties of Mg-doped p-GaN. Journal of Crystal Growth, 2007, 298, 811-814.	1.5	23
300	The effect of InGaN/GaN MQW hydrogen treatment and threading dislocation optimization on GaN LED efficiency. Journal of Crystal Growth, 2007, 298, 740-743.	1.5	23
301	Control of the morphology of InGaN/GaN quantum wells grown by metalorganic chemical vapor deposition. Journal of Crystal Growth, 2007, 300, 324-329.	1.5	38
302	Growth and surface passivation of near-surface InGaAs quantum wells on GaAs (110). Journal of Crystal Growth, 2007, 309, 18-24.	1.5	6
303	Crystal-structure-dependent photoluminescence from InP nanowires. Nanotechnology, 2006, 17, 1580-1583.	2.6	152
304	Multistep method for threading dislocation density reduction in MOCVD grown GaN epilayers. Physica Status Solidi (A) Applications and Materials Science, 2006, 203, R76-R78.	1.8	18
305	Carrier dynamics in strain-induced InGaAsP/InP quantum dots. Physica E: Low-Dimensional Systems and Nanostructures, 2006, 32, 179-182.	2.7	2
306	Nitrogen content of GaAsN quantum wells by in situ monitoring during MOVPE growth. Journal of Crystal Growth, 2006, 290, 345-349.	1.5	6

#	Article	IF	CITATIONS
307	Morphology optimization of MOCVD-grown GaN nucleation layers by the multistep technique. Journal of Crystal Growth, 2006, 292, 26-32.	1.5	22
308	Ge/GaAs heterostructure matrix detector. Nuclear Instruments and Methods in Physics Research, Section A: Accelerators, Spectrometers, Detectors and Associated Equipment, 2006, 563, 17-20.	1.6	3
309	Synchrotron X-ray topography study of defects in epitaxial GaAs on high-quality Ge. Nuclear Instruments and Methods in Physics Research, Section A: Accelerators, Spectrometers, Detectors and Associated Equipment, 2006, 563, 62-65.	1.6	4
310	InAs pixel matrix detectors fabricated by diffusion of Zn in a metal-organic vapour-phase epitaxy reactor. Nuclear Instruments and Methods in Physics Research, Section A: Accelerators, Spectrometers, Detectors and Associated Equipment, 2006, 563, 24-26.	1.6	8
311	Effect of surface states on carrier dynamics in InGaAsP/InP stressor quantum dots. Nanotechnology, 2006, 17, 2181-2186.	2.6	2
312	Characterization of photonic crystal waveguides using Fabry–Perot resonances. Journal of Optics, 2006, 8, S502-S506.	1.5	6
313	Metal Contacts on InN: Proposal for Schottky Contact. Japanese Journal of Applied Physics, 2006, 45, 36-39.	1.5	22
314	Experimental investigation towards a periodically pumped single-photon source. Physical Review B, 2006, 74, .	3.2	21
315	In situ determination of nitrogen content in InGaAsN quantum wells. Journal of Applied Physics, 2006, 100, 013509.	2.5	3
316	Simultaneous determination of indium and nitrogen contents of InGaAsN quantum wells by optical in situ monitoring. Applied Physics Letters, 2006, 89, 231919.	3.3	0
317	Comparison of epitaxial thin layer GaN and InP passivations on InGaAsâ^•GaAs near-surface quantum wells. Applied Physics Letters, 2006, 88, 221112.	3.3	12
318	Catalyst-free growth of In(As)P nanowires on silicon. Applied Physics Letters, 2006, 89, 063119.	3.3	91
319	Synchrotron X-ray topographic study of dislocations and stacking faults in InAs. Journal of Crystal Growth, 2005, 283, 320-327.	1.5	1
320	Synchrotron X-ray topography study of defects in indium antimonide P-I-N structures grown by metal organic vapour phase epitaxy. Journal of Materials Science: Materials in Electronics, 2005, 16, 449-453.	2.2	14
321	Modulation of GaAs(100) surface morphology by ultra-thin MOVPE grown InP layers. AIP Conference Proceedings, 2005, , .	0.4	0
322	High-index-contrast Optical Waveguides on Silicon. AIP Conference Proceedings, 2005, , .	0.4	1
323	Evolution of Self-Assembled InAs/InP Islands into Quantum Rings. Japanese Journal of Applied Physics, 2005, 44, L1323-L1325.	1.5	3
324	Comparison of Ge and GaAs Substrates for Metalorganic Vapor Phase Epitaxy of GaIn(N)As Quantum Wells. Japanese Journal of Applied Physics, 2005, 44, L1475-L1477.	1.5	0

#	Article	IF	CITATIONS
325	Highly Tunable Emission from Strain-Induced InGaAsP/InP Quantum Dots. Japanese Journal of Applied Physics, 2005, 44, L976-L978.	1.5	2
326	Modified self-assembly of InAs islands acting as stressors for strain-induced InGaAs(P)/InP quantum dots. Nanotechnology, 2005, 16, 1630-1635.	2.6	6
327	Low Temperature Growth GaAs on Ge. Japanese Journal of Applied Physics, 2005, 44, 7777-7784.	1.5	28
328	InGaAs/InP Quantum Dots Induced by Self-Organized InAs Stressor-Islands. Japanese Journal of Applied Physics, 2005, 44, L518-L520.	1.5	8
329	Transformation of Self-Assembled InAs/InP Quantum Dots into Quantum Rings without Capping. Nano Letters, 2005, 5, 1541-1543.	9.1	36
330	Structural and optical properties of GalnNAs/GaAs quantum structures. Journal of Physics Condensed Matter, 2004, 16, S3009-S3026.	1.8	11
331	Passivation of GaAs surface by ultrathin epitaxial GaN layer. Journal of Crystal Growth, 2004, 272, 621-626.	1.5	23
332	GaN/GaAs(100) superlattices grown by metalorganic vapor phase epitaxy using dimethylhydrazine precursor. Journal of Crystal Growth, 2004, 270, 346-350.	1.5	3
333	Self-assembled In(Ga) As islands on Ge substrate. Journal of Crystal Growth, 2004, 272, 221-226.	1.5	4
334	Morphology of ultra-thin cubic GaN layers on GaAs(1 0 0) grown by MOVPE with DMHy as nitrogen source. Applied Surface Science, 2004, 222, 286-292.	6.1	5
335	The morphology of an InP wetting layer on GaAs. Applied Surface Science, 2004, 229, 333-337.	6.1	1
336	Optical waveguides on polysilicon-on-insulator. Journal of Materials Science: Materials in Electronics, 2003, 14, 417-420.	2.2	9
337	Growth of GaAs on polycrystalline silicon-on-insulator. Journal of Materials Science: Materials in Electronics, 2003, 14, 403-405.	2.2	1
338	In(Ga)As quantum dots on Ge substrate. Journal of Materials Science: Materials in Electronics, 2003, 14, 349-352.	2.2	5
339	Photoluminescence study of strain-induced GaInNAs/GaAs quantum dots. Journal of Materials Science: Materials in Electronics, 2003, 14, 357-360.	2.2	6
340	Misfit dislocations in GaAsN/GaAs interface. Journal of Materials Science: Materials in Electronics, 2003, 14, 267-270.	2.2	10
341	Effect of post-growth laser treatment on optical properties of Ga(In)NAs quantum wells. IEE Proceedings: Optoelectronics, 2003, 150, 68.	0.8	3
342	Wavelength extension of GalnAs/Galn(N)As quantum dot structures grown on GaAs. Journal of Crystal Growth, 2003, 248, 339-342.	1.5	7

#	Article	IF	CITATIONS
343	Observation of defect complexes containing Ga vacancies in GaAsN. Applied Physics Letters, 2003, 82, 40-42.	3.3	84
344	GalnNAs quantum well structures for 1.55μm emission on GaAs by atmospheric pressure metalorganic vapor phase epitaxy. Journal of Crystal Growth, 2002, 234, 631-636.	1.5	26
345	Self-assembled Galn(N)As quantum dots: Enhanced luminescence at 1.3 μm. Applied Physics Letters, 2001, 79, 3932-3934.	3.3	18
346	Longitudinal Stark Effect in Parabolic Quantum Dots. Japanese Journal of Applied Physics, 2001, 40, 2002-2005.	1.5	6
347	Doping and carrier transport inGa1â^'3xIn3xNxAs1â^'xalloys. Physical Review B, 2001, 64, .	3.2	43
348	Pumping of Quantum Dots with Surface Acoustic Waves. Physica Status Solidi (B): Basic Research, 2001, 224, 703-706.	1.5	0
349	Correlation Effects in Strain-Induced Quantum Dots. Physica Status Solidi (B): Basic Research, 2001, 224, 361-366.	1.5	0
350	Influence of Coulomb and Exchange Interaction on Quantum Dot Magnetoluminescence up to B = 45 T. Physica Status Solidi A, 2000, 178, 263-268.	1.7	3
351	High nitrogen composition GaAsN by atmospheric pressure metalorganic vapor-phase epitaxy. Journal of Crystal Growth, 2000, 221, 456-460.	1.5	53
352	Effects of electron–hole correlation in quantum dots under high magnetic field (up to 45 T). Physica E: Low-Dimensional Systems and Nanostructures, 2000, 7, 346-349.	2.7	2
353	Carrier capture processes in strain-inducedInxGa1â^'xAs/GaAsquantum dot structures. Physical Review B, 2000, 62, 13588-13594.	3.2	7
354	Effects of few-particle interaction on the atomiclike levels of a single strain-induced quantum dot. Physical Review B, 2000, 62, 1592-1595.	3.2	33
355	Effect Of Inp Passivation On Carrier Recombination in InxGa1-xAs/GaAs Surface Quantum Wells. Japanese Journal of Applied Physics, 1999, 38, 1133-1134.	1.5	6
356	Mechanical nanomanipulation of single strain-induced semiconductor quantum dots. Applied Physics Letters, 1999, 75, 358-360.	3.3	17
357	Pauli-blocking imaging of single strain-induced semiconductor quantum dots. Applied Physics Letters, 1999, 74, 3200-3202.	3.3	29
358	Tailoring of Energy Levels in Strain-Induced Quantum Dots. Japanese Journal of Applied Physics, 1999, 38, 1081-1084.	1.5	8
359	Electron-Hole Correlation in Quantum Dots under a High Magnetic Field (up to 45 T). Physical Review Letters, 1999, 83, 4832-4835.	7.8	18
360	Growth and Optical Properties of Strain-induced Quantum Dots. Physica Scripta, 1999, T79, 20.	2.5	4

#	Article	IF	CITATIONS
361	Strain-induced quantum dot superlattice. Physica E: Low-Dimensional Systems and Nanostructures, 1998, 2, 19-22.	2.7	7
362	Hydride vapour phase epitaxy for nanostructures. Materials Science and Engineering B: Solid-State Materials for Advanced Technology, 1998, 51, 238-241.	3.5	6
363	Temperature dependence of carrier relaxation in strain-induced quantum dots. Physical Review B, 1998, 58, R15993-R15996.	3.2	66
364	Magneto-optical properties of strain-inducedInxGa1â^'xAsparabolic quantum dots. Physical Review B, 1998, 57, 9763-9769.	3.2	35
365	Maskless selective growth of InGaAs/InP quantum wires on (100) GaAs. Applied Physics Letters, 1997, 70, 2828-2830.	3.3	8
366	Carrier relaxation dynamics in quantum dots: Scattering mechanisms and state-filling effects. Physical Review B, 1997, 55, 4473-4476.	3.2	119
367	Self-organized InAs islands on (100) InP by metalorganic vapor-phase epitaxy. Surface Science, 1997, 376, 60-68.	1.9	65
368	Synchrotron X-ray topographic study of strain in silicon wafers with integrated circuits. Nuovo Cimento Della Societa Italiana Di Fisica D - Condensed Matter, Atomic, Molecular and Chemical Physics, Biophysics, 1997, 19, 181-184.	0.4	6
369	Ultrafast Relaxation Dynamics in Strain-Induced Quantum Dots. Physica Status Solidi (B): Basic Research, 1997, 204, 251-254.	1.5	14
370	Carrier Relaxation in (Galn)As Quantum Dots. Physica Status Solidi A, 1997, 164, 421-425.	1.7	9
371	Fabrication of GalnAs quantum disks using selfâ€organized InP islands as a mask in wet chemical etching. Applied Physics Letters, 1996, 69, 4029-4031.	3.3	3
372	Synchrotron X-ray topographic analysis of the impact of processing steps on the fabrication of AlGaAs/InGaAs p-HEMT's. IEEE Transactions on Electron Devices, 1996, 43, 1085-1091.	3.0	0
373	Fabrication and photoluminescence of quantum dots induced by strain of self-organized stressors. Solid-State Electronics, 1996, 40, 601-604.	1.4	15
374	Metalorganic vapor phase epitaxial growth of AlGaSb and AlGaAsSb using all-organometallic sources. Journal of Crystal Growth, 1996, 169, 417-423.	1.5	17
375	Red luminescence from strainâ€induced GaInP quantum dots. Applied Physics Letters, 1996, 69, 3393-3395.	3.3	17
376	Enhanced optical properties of in situ passivated nearâ€ s urface AlxGa1â^'xAs/GaAs quantum wells. Applied Physics Letters, 1996, 68, 2216-2218.	3.3	32
377	Zeeman Effect in Parabolic Quantum Dots. Physical Review Letters, 1996, 77, 342-345.	7.8	99
378	Recombination processes in strain-induced InGaAs quantum dots. Nuovo Cimento Della Societa Italiana Di Fisica D - Condensed Matter, Atomic, Molecular and Chemical Physics, Biophysics, 1995, 17, 1699-1703.	0.4	7

#	Article	IF	CITATIONS
379	Optical spectroscopy of bragg confined transitions in a superlattice with multiquantum barriers. Solid State Communications, 1995, 93, 525-528.	1.9	3
380	Growth of high-quality GaSb by metalorganic vapor phase epitaxy. Journal of Electronic Materials, 1995, 24, 1691-1696.	2.2	20
381	Luminescence from excited states in strain-inducedInxGa1â^'xAs quantum dots. Physical Review B, 1995, 51, 13868-13871.	3.2	174
382	Strainâ€induced quantum dots by selfâ€organized stressors. Applied Physics Letters, 1995, 66, 2364-2366.	3.3	88
383	Selfâ€organized InP islands on (100) GaAs by metalorganic vapor phase epitaxy. Applied Physics Letters, 1995, 67, 3768-3770.	3.3	70
384	Modeling, fabrication, and characterization of 1.43-um InGaAsP/InP separate confinement heterostructure multiple quantum-well lasers. Optical Engineering, 1995, 34, 2527.	1.0	2
385	Selective growth of InGaAs on nanoscale InP islands. Applied Physics Letters, 1994, 65, 1662-1664.	3.3	93
386	Growth of GaInAsSb using tertiarybutylarsine as arsenic source. Journal of Crystal Growth, 1994, 145, 492-497.	1.5	30
387	Photoluminescence of buried InGaAs grown on nanoscale InP islands by MOVPE. Journal of Crystal Growth, 1994, 145, 988-989.	1.5	3
388	Growth and characterization of a GaAs/AlAs superlattice with variable layer thicknesses. Journal of Electronic Materials, 1994, 23, 465-470.	2.2	0
389	Fabrication of nanostructures using MBE and MOVPE. Physica Scripta, 1994, T54, 241-243.	2.5	1
390	Interference effects in photoreflectance of epitaxial layers grown on semiâ€insulating substrates. Applied Physics Letters, 1993, 63, 2863-2865.	3.3	30
391	Praseodymium Dioxide Doping of In1â^'xGaxAsyP1â^'y Epilayer Grown with Liquid Phase Epitaxy. Materials Research Society Symposia Proceedings, 1993, 301, 27.	0.1	2
392	Photoreflectance study of photovoltage effects in GaAs diode structures. Applied Physics Letters, 1992, 60, 2110-2112.	3.3	17
393	High-speed InGaAsP/InP multiple-quantum-well laser. IEEE Photonics Technology Letters, 1992, 4, 673-675.	2.5	25
394	X-ray diffraction analysis of superlattices grown on misoriented substrates. Journal of Crystal Growth, 1991, 114, 569-572.	1.5	7
395	Study of GaAs/AlGaAs and InGaAs/InP quantum well structures using low-field transverse electroreflectance. , 1990, 1286, 300.		0
396	Photoreflectance studies of InGaAs/InP superlattices. , 1990, 1286, 238.		0

#	Article	IF	CITATIONS
397	Roomâ€ŧemperature observation of impurity states in bulk GaAs by photoreflectance. Journal of Applied Physics, 1989, 65, 2556-2557.	2.5	24
398	Synchrotron section topographic study of defects in InP substrates and quaternary laser structures. Journal of Crystal Growth, 1989, 96, 881-887.	1.5	3
399	Enhanced luminescence of near-surface quantum wells passivated in situ by InP. , 0, , .		0
400	Optical properties of self-organized InGaAs/InP dots. , 0, , .		1
401	Effect of InP passivation on carrier recombination in In/sub x/Ga/sub 1-x/As/GaAs surface quantum wells. , 0, , .		0
402	Vacancy-type defects in GaAsN grown by metalorganic vapor phase epitaxy. , 0, , .		0
403	Growth of self-assembled GaIn(N)As quantum dots by atmospheric pressure metalorganic vapor phase epitaxy. , 0, , .		0
404	Photonic crystal slabs with ring-shaped holes in a triangular lattice. , 0, , .		2
405	Thermoelectric Characteristics of InAs Nanowire Networks Directly Grown on Flexible Plastic Substrates. ACS Applied Energy Materials, 0, , .	5.1	3